Spin-disorder effects in the electrical resistivity of Ni-based amorphous alloys

W. H. Kettler and M. Rosenberg

Ruhr-Universität Bochum, Experimentalphysik VI, D-4630 Bochum 1, West Germany
(Received 2 May 1988; revised manuscript received 28 December 1988)

The electrical resistivity ρ of Ni-based ferromagnetic amorphous $Ni_{80-x}Fe_xB_{16}Si_4$ and $Ni_{77-x}Fe_xB_{13}Si_{10}$ alloys with $x=0$ to 19 and $x=0$ to 15.4, respectively, was measured in the temperature range 1.5–300 K. The temperature-dependent part of the magnetic contribution ρ_{mag} to the total resistivity was obtained by subtracting from the measured ρ at each temperature the electrical resistivity of the corresponding Pauli paramagnetic Ni parent alloy ($x=0$). It is found that at low-temperatures ρ_{mag} has a $T^{3/2}$ dependence, which near the Curie point T_C changes to a linear dependence. Above the Curie temperature, ρ_{mag} still increases saturating only at temperatures well above T_C. At low temperatures the $T^{3/2}$ term of ρ_{mag} decreases monotonously with increasing Fe concentration, while the linear $\rho_{mag}(T)$ term for $T \lesssim T_C$ is nearly independent of the Fe content. In the ferromagnetic range, both the temperature and the concentration dependence of ρ_{mag} are found to be in quantitative agreement with the predictions of the spin-disorder model adapted to the peculiarities of the amorphous structure. It is also found that quenched disorder does not have any noticeable effect on the characteristic resistivity ρ_0^c associated with the strength of sd exchange interaction.

I. INTRODUCTION

In crystalline and amorphous ferromagnetic metals and alloys, there is a contribution ρ_{mag} to the electrical resistivity ρ which is closely associated with the magnetic behavior. For instance, the onset of ferromagnetic ordering results in a sharp break in $\rho(T)$ at the Curie temperature T_C, as well as a considerably enhanced (compared to that of nonmagnetic materials) temperature coefficient of resistivity (TCR) (Refs. 1–5) $\alpha_T = d \ln\rho/dT$. In crystalline ferromagnets the interaction of the conduction electrons with the collective excitations (magnons) of the localized spin system at low temperatures gives rise to a T^2 power law for ρ_{mag} (Refs. 6–8), which has also been observed in some Fe-rich ferromagnetic metallic glasses[9] with a proportionality coefficient of roughly the same order of magnitude. However, since in amorphous metals electron-phonon scattering also leads to a T^2 power law for ρ at low temperatures,[10] experimental identification of these distinct contributions is difficult.[9] On the other hand, measurements have also inferred a $T^{3/2}$ power law for ρ_{mag} in the spin-wave region,[5,11] which has its origin in the amorphous structure and agrees with the theoretical predictions.[12]

Despite the plethora of experimental data on the resistivity of ferromagnetic amorphous alloys,[1] the identification of the magnetic contribution to the total resistivity in these materials, as well as the question of the effect of quenched disorder on the magnetic scattering mechanism, are still the subject of much discussion. Besides the above-mentioned experimental difficulties in the low-temperature region, the considerable number of simplifying assumptions in most theoretical models[12,13] further hinders a straightforward comparison between theory and experiment.

Transport properties of ferromagnetic materials are in-

trinsically determined by the properties of the electron-band structure, which, in contrast to that of nonmagnetic metals, is characterized by the superposition of a broad s band and a narrow d band with common Fermi energy.[14] Due to their large effective mass the d state do not contribute directly to the charge transport. However, in strong ferromagnetic materials the cross section for potential scattering of $s\uparrow$ and $s\downarrow$ electrons into hole states in the d band can differ considerably. Besides the additive contributions of the individual scattering mechanisms, the superposition of potential scattering and spin scattering gives rise to an additional (mixing) term in the total resistivity, causing strong deviations from Matthiessen's rule.[14,15] The ratio of the partial residual resistivities of the s-sub-bands, $\alpha = \rho_0^{\downarrow}/\rho_0^{\uparrow}$, which is obtainable from measurements of the spontaneous magnetic resistivity anisotropy, determines the order of magnitude of this additional contribution to ρ. This two-current conduction (TCC) model originally suggested by Mott[16] and developed by Fert and Campbell,[14] has turned out to be remarkably successful in explaining the transport properties of crystalline ferromagnets. Up to now these ideas have not been utilized for studying the resistivity in amorphous ferromagnets. The difficulty is that as evidenced by recent numerical studies,[17,18] the basic assumption of the TCC model that the d states do not participate directly in the transport processes do not necessarily apply to the $3d$ transition metal-based amorphous alloys. Therefore great caution should be exercised while applying the TCC model to these materials.

The latter remarks considerably restrict the choice of amorphous systems suitable for a quantitative test of the existing theoretical transport models. To avoid complications associated with the mixing term in the total resistivity, one should first investigate systems exhibiting weak itinerant ferromagnetism in the sense of Stoner's

criterion and hence having negligible deviations from Matthiessen's rule. The Ni-rich amorphous $Ni_{77-x}Fe_xB_{13}Si_{10}$ and $Ni_{80-x}Fe_xB_{16}Si_4$ alloy series with compositions close to the percolation threshold, x_c, are particularly suitable for this purpose, since the conductivity of the Ni parent alloys $(x=0)$ is expected to be dominated by the s-band contributions.[17] While in both of these systems the Ni parent alloys are Pauli paramagnetic, substitution of a few at. %Ni by Fe gives rise to long-range ferromagnetic ordering. Under appropriate conditions, the resistivity of the Ni parent alloys can be taken to be approximately the nonmagnetic part in the ferromagnetic phase and used for identification of the magnetic contribution $\rho_{mag}(T)$ from the total resistivity, so that a quantitative analysis of ρ_{mag} within the framework of appropriate theoretical models is possible.

II. EXPERIMENTAL DETAILS

Amorphous $Ni_{80-x}Fe_xB_{16}Si_4$ $(x \leq 19)$ and $Ni_{77-x}Fe_xB_{13}Si_{10}$ $(x \leq 15.4)$ alloy ribbons having a cross section of about 0.02×2 mm^2 were prepared by the rotating drum technique in an argon atmosphere. The amorphous nature of the alloy ribbons was verified by x-ray diffraction technique using Mo $K\alpha$ radiation. Throughout this paper nominal compositions have been used. A quantitative analysis of the actual compositions of these alloys by means of a microprobe did not show any deviations from the nominal composition of the ingots within the uncertainty of the measurement (1 at. %).

Electrical resistivity ρ was measured in the temperature range 1.5–300 K by means of a four-probe ac compensation method.[5] The experimental setup for these measurements could resolve a few ppm change in the resistivity with ease. While the voltage contacts (~ 20 mm apart) were formed by thin gold wires of 25 μm diameter soldered to the sample (length ~ 30 mm) with a low-melting, nonsuperconducting, soldering material $(Bi_{45}Cd_{55})$, the current contacts were made by soldering a bundle of several thin gold wires to the ends of the ribbons by means of In soldering material. During the soldering procedure, special care has been taken to avoid structural relaxation, or in the worst case, crystallization of the amorphous ribbons. The ribbons were placed on a rectangular sapphire plate, and the gold wires were then soldered to the conducting silver contacts which have been diffused into the wafer at elevated temperatures. To avoid stress-induced effects in the course of measurement, no grease was used to affix the samples to the sapphire support. The tensile gold wires allowed for changes in the sample dimensions during thermal cycling. The sample temperature was monitored by calibrated Pt- and Ge-resistance thermometers placed underneath the wafer.

The average cross-sectional area of each sample was deduced from the weight, length, and density. The density of the metallic glasses was derived from the density function given by Aso et al.[19] The accuracy in the absolute values of ρ can be estimated to be better than 5%, which can be ascribed mainly to the uncertainty in the density data. During thermal cycling, changes in the sample dimensions can occur because of finite thermal ex-

pansion. Due to the lack of information about the thermal expansion coefficients in the amorphous alloys investigated, no corrections have been made, so that the $\rho(T)$ data, which have been normalized to the sample dimensions at $T_0 = 273.15$ K, should be taken as apparent resistivity.

III. EXPERIMENTAL RESULTS AND DATA ANALYSIS

The temperature variation of the normalized resistivity ratio $r(T) = \rho(T)/\rho(T_0)$, where $T_0 = 273.15$ K is the ice point, along with the corresponding derivative $r'(T) = dr(T)/dT$ in the temperature range 1.5–300 K for several amorphous $Ni_{80-x}Fe_xB_{16}Si_4$ $(x \leq 19)$ and $Ni_{77-x}Fe_xB_{13}Si_{10}$ $(x \leq 15.4)$ alloys are shown in Figs. 1 and 2. The salient features of the $r(T)$ and $r'(T)$ curves can be summarized as follows: (i) the total fractional change $\Delta\rho/\rho$ in resistivity within the investigated temperature range increases progressively with increasing Fe concentration, reaching the exceptionally large value of about 12% for $x = 11$ at. %Fe, (ii) at low temperatures $(T < 11$ K), $\rho(T)$ goes through a well-defined resistivity minimum at a temperature T_{min} (see Table I), (iii) above T_{min} the increment of ρ with increasing temperature fol-
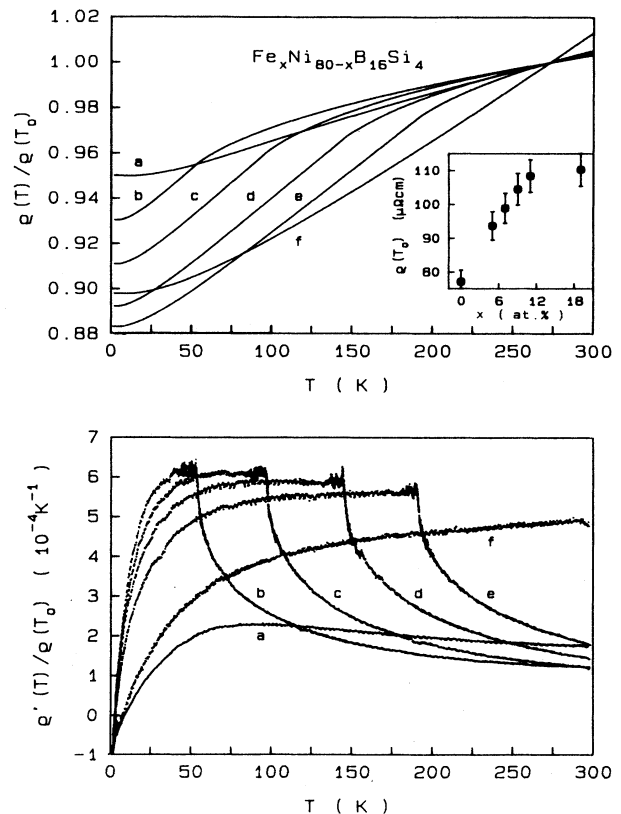
FIG. 1. Temperature dependence of the normalized resistivity ratio $\rho(T)/\rho(T_0)$ (above) and the corresponding derivative $\rho'(T)/\rho(T_0)$ (below) of amorphous $Ni_{80-x}Fe_xB_{16}Si_4$ alloys for (a) $x = 0$, (b) 5, (c) 7, (d), 9, (e) 11, and (f) 19, where $T_0 = 273.15$ K is the ice point. The inset (above) depicts the concentration dependence of $\rho(T_0)$.
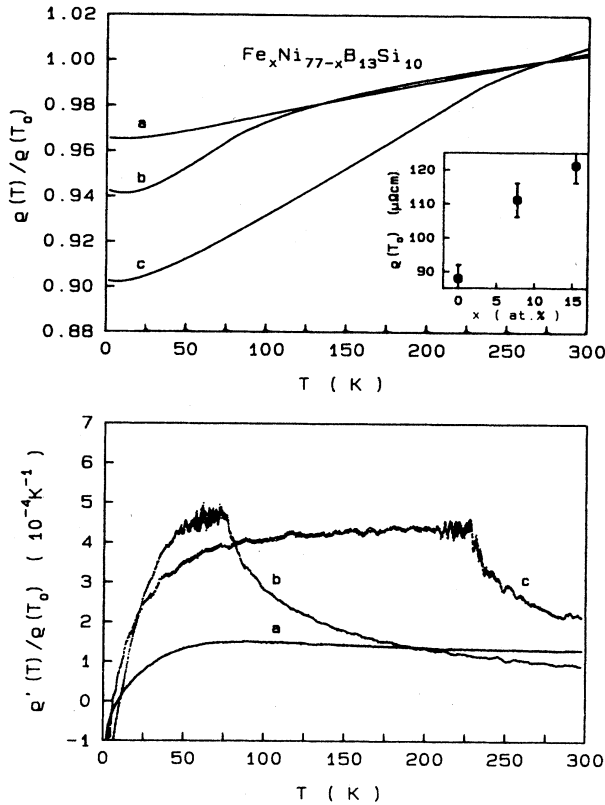
FIG. 2. Temperature dependence of the normalized resistivity ratio $\rho(T)/\rho(T_0)$ (above) and the corresponding derivative $\rho'(T)/\rho(T_0)$ (below) of amorphous $Ni_{77-x}Fe_xB_{13}Si_{10}$ alloys for (a) $x=0$, (b) 7.7 and (c) 15.4, where $T_0=273.15$ K is the ice point. The inset (above) depicts the concentration dependence of $\rho(T_0)$.

lows approximately a T^n power law with $n \approx 1.5-2$, which for the ferromagnetic compositions in the vicinity of the Curie-point T_C changes to a linear ($n=1$) dependence, (iv) the onset of long-range ferromagnetic ordering leads to a break in the $\rho(T)$ behavior, at which point the

slope $d\rho/dT$ rapidly decreases with increasing temperature, and (v) far above the Curie point, in the paramagnetic range, ρ again varies linearly with temperature and has a slope such that for all investigated compositions within both alloy series seems to converge to the same value.

The unusually large change in $\rho(T)$ within the investigated temperature range for compositions with $x > x_c$ and the marked concentration dependence of $\Delta\rho/\rho$ certainly cannot be explained solely by the diffraction model,[10] which completely disregards the magnetic state of the glassy alloys and attributes the magnitude and temperature variation of ρ to the scatttering of the conduction electrons by the disordered ion cores with a muffin-tin potential. The observed anomaly in $\rho(T)$ at the Curie temperature indicates that in these *diluted* amorphous ferromagnets the magnetic state, which close to the percolation threshold is subject to dramatic changes, exerts a strong influence on the electronic charge transport. Contrary to the results previously obtained for *concentrated* amorphous ferromagnets[9] exhibiting high Curie temperatures, in the metallic glasses here the magnetic contribution to ρ is no longer small compared to that of the (incremental) structural contribution, thus rendering a unique identification of $\rho_{mag}(T)$ possible.

Only within the localized picture of metallic magnetism and under the assumption of dominant s-band contribution to the conductivity, a simple quantitative analysis of the magnetic contribution $\rho_{mag}(T)$ to the total resistivity can be performed without using any particular transport model, although one has to make an assumption which can only be justified by the experimental results. This assumption pertains to the applicability of Matthiessen's rule which asserts the additivity of the resistivities which would be expected if each of the physically distinguishable scattering mechanisms were present alone. Accordingly, the total resistivity

$$\rho(T)=\rho_0+\rho_{ph}(T)+\rho_{mag}(T)+\Delta(T) \qquad (1)$$

of a ferromagnetic material is composed of four contribu-

TABLE I. Compilation of some relevant experimental quantities of resistivity behavior in the amorphous $Ni_{80-x}Fe_xB_{16}Si_4$ and $Ni_{77-x}Fe_xB_{13}Si_{10}$ alloy systems. The density data have been calculated utilizing the function derived by Aso *et al.* (Ref. 19) for this class of amorphous alloys.

Material	Density (g/cm³)	(273.15 K) (μΩ cm)	α_T (273.15 K) (ppm/K)	T_{min} (K)	T_C (K)
$Ni_{80}B_{16}Si_4$	8.35	77.12±3.5	125.6±2	10.07±0.1	
$Fe_1Ni_{79}B_{16}Si_4$	8.33	81.76±3.7	157.1±2	16.12±0.2	
$Fe_2Ni_{78}B_{16}Si_4$	8.32	87.69±3.9	144.5±2	6.08±0.2	
$Fe_3Ni_{77}B_{16}Si_4$	8.31	88.00±3.9	124.8±2	7.23±0.2	
$Fe_5Ni_{75}B_{16}Si_4$	8.28	93.63±4.2	125.6±2	3.81±0.1	54.7±0.3
$Fe_7Ni_{73}B_{16}Si_4$	8.26	98.83±4.4	130.7±2	3.90±0.1	98.0±0.3
$Fe_9Ni_{71}B_{16}Si_4$	8.23	104.43±4.7	162.0±2	3.65±0.1	146.3±0.3
$Fe_{11}Ni_{69}B_{16}Si_4$	8.20	108.33±4.9	208.2±2	4.17±0.1	191.9±0.3
$Fe_{19}Ni_{61}B_{16}Si_4$	8.10	110.24±4.9	483.8±2	9.06±0.1	> 300
$Ni_{77}B_{13}Si_{10}$	8.12	87.93±4.0	130.3±2	9.30±0.2	
$Fe_{7.7}Ni_{69.3}B_{13}Si_{10}$	8.02	111.12±5.0	100.0±2	10.50±0.2	75.0±0.3
$Fe_{15.4}Ni_{61.6}B_{13}Si_{10}$	7.92	121.19±5.0	237.1±2	6.20±0.2	299.1±0.3

tions: a temperature independent residual resistivity ρ_0 (which can also contain a magnetic contribution), two temperature-dependent terms $\rho_{ph}(T)$ and $\rho_{mag}(T)$ caused by electron-phonon (e-ph) interaction and scattering of the conduction electrons on the disordered local magnetic moments, respectively, while the fourth term $\Delta(T)$ is due to deviations from Matthiessen's rule. This composition of ρ implies that in the limit $T \to 0$ K both of the temperature-dependent terms $\rho_{ph}(T)$ and $\rho_{mag}(T)$ vanish. Above the Curie point within the spin-disorder model, a constant magnetic contribution $[\rho_{mag}(T \gg T_c) = \text{const}]$ is expected. On the other hand, experimental[1] and theoretical[10] results show that the phonon contribution $\rho_{ph}(T)$ has a linear T dependence for $T \gtrsim \Theta_D$ ($= $Debye temperature). Hence, assuming $\Delta(T)$ to be negligibly small, extrapolation of the high temperature ($T \gg T_c$, $T \gtrsim \Theta_D$) part of the experimental resistivity curve to $T \to 0$ K leads to

$$\rho_0^* = \rho_0 + \rho_{mag}(T \gg T_c) , \qquad (2)$$

from which the constant paramagnetic spin-disorder resistivity $\rho_{mag}(T \gg T_c)$ can be deduced.

Another procedure for obtaining ρ_{mag} follows from a comparison of the transport properties of the magnetic and the isostructural nonmagnetic materials. Assuming again the validity of Matthiessen's rule, the total resistivity of the magnetic (M) and nonmagnetic (NM) samples can be expressed as

$$\rho^M(T) = \rho_0^M + \rho_{ph}^M(T) + \rho_{mag}(T) + \Delta^M(T) , \qquad (3a)$$

$$\rho^{NM}(T) = \rho_0^{NM} + \rho_{ph}^{NM}(T) + \Delta^{NM}(T) . \qquad (3b)$$

Subtracting the experimentally known residual resistivity, Eqs. (3a) and (3b) can be written as

$$\rho_{red}^M(T) = \rho^M(T) - \rho_0^M$$
$$= \rho_{ph}^M(T) + \rho_{mag}(T) + \Delta^M(T) \qquad (4a)$$

and

$$\rho_{red}^{NM}(T) = \rho^{NM}(T) - \rho_0^{NM} = \rho_{ph}^{NM}(T) + \Delta^{NM}(T) . \qquad (4b)$$

Since $\rho_{ph}^{NM}(T \to 0 \text{ K}) = \rho_{ph}^M(T \to 0 \text{ K}) = \rho_{mag}(T \to 0 \text{ K}) = 0$, from the difference

$$\rho^*(T) = \rho_{red}^M(T) - \rho_{red}^{NM}(T)$$
$$= \rho_{ph}^M(T) - \rho_{ph}^{NM}(T) + \Delta^M(T) - \Delta^{NM}(T) + \rho_{mag}(T) , \qquad (5)$$

one can again obtain the paramagnetic spin-disorder contribution from an extrapolation of the high-temperature portion of $\rho^*(T)$. The present analysis allows the identification of magnetic resistivity contributions for the whole ferromagnetic range, provided that $[\rho_{ph}^m(T) - \rho_{ph}^{NM}(T)] \ll \rho_{mag}(T)$ and that deviations from Matthiessen's rule can be neglected.

Although the procedures for identifying the magnetic resistivity contributions described above have been successfully applied to a large number of crystalline alloys,[20-22] up to now they have not found favor in the analysis of resistivity data for amorphous ferromagnets. In the following, we show that a similar procedure can be applied to amorphous systems.

Before proceeding to discuss our experimental results in the light of above-mentioned methods for measuring magnetic resistivity contributions, it is appropriate to make a few comments on the assumptions inherent in this type of analyses. Alloying can affect the resistivity in several ways. In the dilute limit, the impurities act as local disturbances in the "ideal" amorphous structure of the host alloy, and as such contribute to the residual resistivity. Beyond the dilute limit, alloying may significantly alter the electronic band structure, changing thereby those parameters which partially determine the resistivity of the host alloy. Particularly in amorphous alloys, small changes in the Fermi wave vector, k_F, may result in drastic changes in the nonmagnetic resistivity contribution, and may even reverse the sign of its temperature coefficient α_T (Ref. 10). Besides, alloying is often accompanied by changes in the elastic properties and thus also modifications in the phonon spectrum, which can affect the "ideal" resistivity. In contrast to crystalline metals for which the (nonmagnetic) normalized resistivity $\rho_{ph}(T)/\rho_{ph}(\Theta_D)$ falls approximately on a single universal curve, the situation for amorphous metals turns out to be more complicated, owing to the absence of such a universal relationship.

In view of recent specific-heat measurements[23,24] performed on the same alloy series as those under consideration, the last possibility stated above can be ruled out. These investigations indicate that, on account of a roughly concentration-independent Debye-temperature θ_D, the details of the phonon spectrum are not significantly altered over the range of purity studied here. Significant changes of the host resistivity may arise only from a shift of the Fermi wave vector k_F on alloying. Within the free electron approximation, the shift of $k_F \simeq k_F^0 [1 - (x/3)(\Delta Z/Z_0)]$ depends upon the difference $\Delta Z = Z_0 - Z$ of the effective valences between the host (Z_0 for $Ni_{80}B_{16}Si_4$ and $Ni_{77}B_{13}Si_{10}$) and the impurity (Z for Fe). Consequently, the range of applicability of the ρ_{mag} identification process is restricted to appropriately low Fe concentrations.

Another complication is that on one hand in all the alloys studied an additional scattering mechanism becomes effective at low temperatures ($T < 11$ K) leading to an increase in the resistivity with decreasing temperature, and on the other hand, the experimental results show strong evidence of the persistence of the temperature dependence of ρ_{mag} far into the paramagnetic range. Therefore, both the determination of the residual resistivity and the extrapolation of the high-temperature range are subject to a certain inaccuracy.

Owing to the negligible changes below the minimum, the residual resistivity ρ_0^* can be set equal to $\rho(T_{min})$. The problem of extrapolating ρ^* from the high-temperature range is more difficult. While $r'(T)$ for the composition $x \leq 7$ of the $B_{16}Si_{4^-}$ ($x = 7.7$ of the $B_{13}Si_{10^-}$) system is almost constant (i.e., $\rho \sim T$), for higher Fe concentrations it exhibits a marked curvature even at

$T = 300$ K. In fact, we found $r'(T)$ for different composi-
tions converge to that of $x = 5$ ($x = 7.7$ for the second
system) at sufficiently high temperatures. Thus, in order
to obtain ρ_0^*, these high-temperature resistivity curves
(which have been generated by linear extrapolation of the
dr/dT data) can to a good approximation be extrapolated
to $T = 0$ K using the slope of that of $x = 5$ ($x = 7.7$).
Thereafter ρ_{mag} can be determined using Eq. (2). The re-
sidual $\rho^*(0)$ in the subtraction method is obtained from
an analysis of the limiting low-temperature behavior of
ρ_{mag}.

Figure 3 depicts the constant paramagnetic resistivity
ρ_{mag} at high temperature in both alloy systems studied
here as a function of Fe concentration. The error bars re-
sult from the absolute accuracy of the electrical resistivi-
ty, and the scatter in the data due to the two: namely, ex-
trapolation and subtraction methods used. We note that
in both systems $\rho_{mag}(T \gg T_c)$ exhibits within the error
limits a linear dependence on Fe concentration with a
slope of (1.03 ± 0.07) $\mu\Omega$ cm/at. %Fe for the $B_{16}Si_4$ and
(0.90 ± 0.10) $\mu\Omega$ cm/at. %Fe for the $B_{13}Si_{10}$ alloy series,
respectively.

The results of the subtraction analysis are shown in
Fig. 4, where the temperature-dependence part of ρ_{mag} as
a function of temperature has been plotted. In both sys-
tems the corresponding Pauli paramagnetic composition
[$Ni_{80}B_{16}Si_4$ (Ref. 25) and $Ni_{77}B_{13}Si_{10}$ (Ref. 26), respective-
ly] serves as the nonmagnetic basis alloy. The curves in
Fig. 4 exhibit a marked change in slope at the ferromag-
netic ordering temperature, T_c, determined from a de-
tailed magnetization study,[25] which within the error lim-
its specified in Table I corresponds to the temperature
where the derivative dr/dT attains its maximum. Satura-
tion of ρ_{mag} can only be observed far above T_c, where the
curves are essentially flat. Above $T \gtrsim 2T_c$, there is no evi-
dence of any temperature- or concentration-dependent
scattering mechanism, which cannot be accounted for by
that of the corresponding Ni parent alloy. The slight de-

crease of ρ_{mag} with temperature for $T \gg T_c$ at low Fe
concentrations should not be ascribed to deviations from
Matthiessen's rule, but rather to the resistivity of the
basis alloy ($Ni_{80}B_{16}Si_4$), which at room temperature ex-
hibits a somewhat higher TCR than that of the ferromag-
netic compositions. As can be seen from the increase of
ρ_{mag} between T_c and the flat portion of the curves, short-
range magnetic correlations of the spin system can be
detected well into the paramagnetic range. Below T_c, to
a good approximation ρ_{mag} is a linear function of temper-
ature with a slope B (see Table II) which for within both
alloy series studied is roughly independent on composi-
tion. Careful examination of the low-temperature behav-
ior reveals an asymptotic $T^{3/2}$ power law for ρ_{mag} as
$T \rightarrow 0$ K with a proportionality constant A (see Table II),
which progressively decreases with increasing Fe concen-
tration. The magnitudes for both A and B are compara-
ble to those of crystalline diluted ferromagnetic al-
loys.[20-22]

FIG. 3. Variation of the constant paramagnetic resistivity
contribution $\rho_{mag}(T \gg T_c)$ of amorphous $Ni_{80-x}Fe_xB_{16}Si_4$
(closed circles) And $Ni_{77-x}Fe_xB_{13}SI_{10}$ alloys (crosses) with com-
position. The least-squares-fit straight lines through the data
points are also shown.
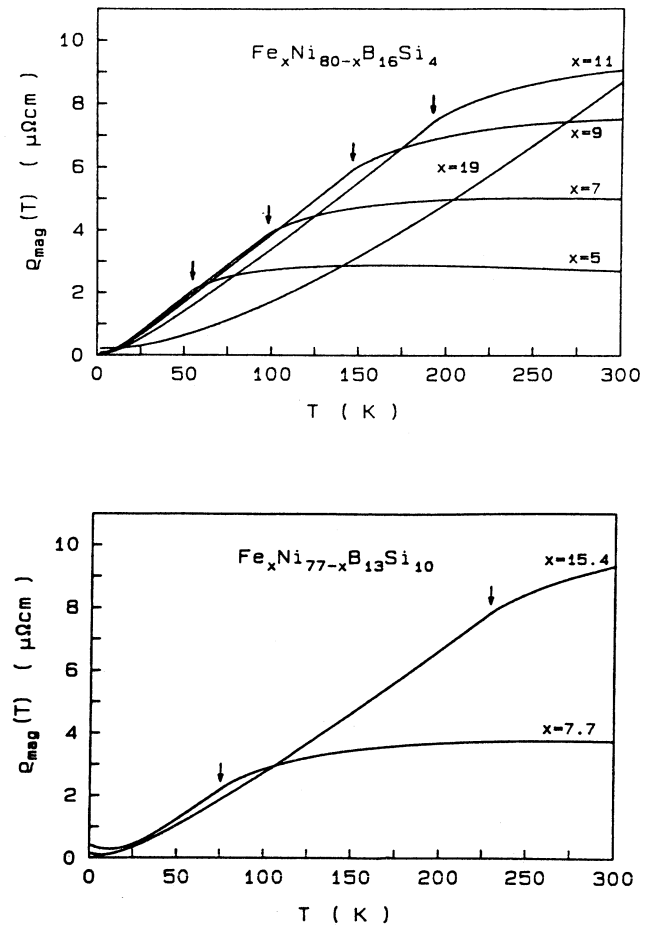
FIG. 4. Temperature dependence of the separated incremen-
tal magnetic resistivity contribution $\rho_{mag}(T)$ of amorphous
$Ni_{80-x}Fe_xB_{16}Si_4$ (above) and $Ni_{77-x}Fe_xB_{13}Si_{10}$ alloys (below).
The arrows locate the respective transition temperatures T_c.

TABLE II. Parameters characterizing the magnetic and electronic properties of various magnetically diluted amorphous $Ni_{80-x}Fe_xB_{16}Si_4$ and $Ni_{77-x}Fe_xB_{13}Si_{10}$ alloys. Numbers in the square brackets denote extrapolated values, while parentheses enclose the temperature range used for the fit of the respective parameter. Average local magnetic moments μ, μ_{Fe}, μ_{Ni}, and stiffness constant D of the amorphous $B_{13}Si_4$-alloy series have been taken from Ref. 32. Corresponding values for μ_{Fe} and μ_{Ni} of the amorphous $B_{13}Si_{10}$ alloys have been calculated by means of published hyperfine field (HF) and magnetization (μ) (Ref. 26) utilizing the HF coupling parameters determined in Ref. 32 for the a-$Ni_{80-x}Fe_xB_{16}Si_4$ system (for details see text).

Material	μ/TM (μ_B)	μ_{Fe} (μ_B)	μ_{Ni} (μ_B)	D (MeV Å^2)	$\rho_{mag}(T \gg T_c)$ ($\mu\Omega$ cm)	$a_3(2k_F)$ Expt.	Calc.	$\rho_{mag}(0)$ ($\mu\Omega$ cm)	B ($n\Omega$ cm/K)	A ($n\Omega$ cm/K$^{3/2}$) Expt.	Calc.
$Fe_5Ni_{75}B_{16}Si_4$	0.215	1.80	0.109	24	3.39±0.2	4.0	5.8	1.1	43.5±1.2 (35–54 K)	6.05±0.19 (11–26 K)	2.83
$Fe_7Ni_{73}B_{16}Si_4$	0.30	1.84	0.152	35	5.49±0.3	2.4	4.4	1.5	42.9±1.2 (60–97 K)	5.65±0.17 (10–30 K)	1.58
$Fe_9Ni_{71}B_{16}Si_4$	0.38	1.87	0.191	42	7.82±0.3	1.9	3.7	2.0	44.8±1.2 (90–145 K)	5.28±0.16 (8–30 K)	1.26
$Fe_{11}Ni_{69}B_{16}Si_4$	0.46	1.88	0.234	51	9.34±0.3	1.8	3.2	2.6	45.6±1.2 (140–191 K)	4.26±0.13 (11–34 K)	1.01
$Fe_{19}Ni_{61}B_{16}Si_4$	[0.79]	[1.88]	[0.45]	[86.4]	[16.1]		2.0	6.2		1.74±0.09 (66–202 K)	0.64
$Fe_{7.7}Ni_{69.3}B_{13}Si_{10}$	0.177	1.715	0.006	40	3.82±0.3	5.5	12.2	1.3	38.7±0.5 (60–75 K)	3.49±0.13 (28–55 K)	1.97
$Fe_{15.4}Ni_{61.6}B_{13}Si_{10}$	0.581	1.731	0.294	59	10.74±0.5	2.0	2.6	3.6	40.7±0.5 (180–225 K)	2.95±0.12 (11–46 K)	0.93

IV. DISCUSSION

The similarity between the temperature and concentration dependence of ρ_{mag} of the amorphous Fe-Ni alloy series studied here and that of crystalline ferromagnetic alloys suggests a common origin for the potentially significant electron scattering mechanisms, so that it is reasonable to invoke known thoeretical models for crystalline ferromagnetic alloys when seeking an explanation for the present results. In particular, the rough agreement in the paramagnetic resistivity contribution per Fe atom in the investigated glassy alloys with that in crystalline Fe (Refs. 27 and 28) indicates that the frozen disorder does not exert any noticeable influence on the dominant magnetic scattering mechanisms. However, before coming to the main concern of this paper and embarking upon a detailed investigation of the separated magnetic resistivity contribution $\rho_{mag}(T)$, one has to provide a thorough theoretical justification for the decomposition of the resistivity data described in the preceding section as to pinpoint the attainable accuracy for $\rho_{mag}(T)$.

Our procedure for obtaining ρ_{mag} is mainly based on the assumption of dominant s-band contributions to the conductivity and the applicability of the extended Faber-Ziman (EFZ) theory to the amorphous alloy systems involved. Recent numerical studies[17,18] on the electronic charge transport in liquid and amorphous $3d$ transition metals and alloys have indicated substantial contributions of d electrons to conductivity in these materials, and hence raised some doubts on the applicability of the diffraction model to systems whose Fermi energy is located within the d band. Nevertheless, several reasons can be adduced for the applicability of EFZ theory to the Ni parent compositions of the present amorphous alloy

series. Theoretical investigations on resistivity behavior demonstrate not only that, e.g., in liquid Ni, the s-band contribution should dominate the conductivity,[17] but the EFZ theory gives a value for ρ (~ 74 $\mu\Omega$ cm) in good agreement[29] with that observed experimentally (~ 83 $\mu\Omega$ cm). Moreover, $\rho(T_0)$ of the (Pauli paramagnetic) amorphous $Ni_{80}B_{16}Si_4$ and $Ni_{77}B_{13}Si_{10}$ parent alloys is close to that of liquid Ni, so that it is not unexpected that both the magnitude of resistivity and its variation with temperature can be quanitatively explained on the basis of the EFZ theory if one follows the approach adopted by Cote and Meisel[10] for explaining the $\rho(T)$ behavior in a-$Ni_{100-x}P_x$ alloys. In particular, from the proposed transport models discussed so far, only the latter approach can reproduce the experimentally observed asymptotic quadratic and linear temperature dependences for ρ at low $(T \ll \Theta_D)$ and high $(T \gtrsim \Theta_D)$ temperatures, respectively. Keeping in view the experimental finding that within the composition range studied in the present work, the Debye-temperature Θ_D of the amorphous alloys does not change significantly,[23,24] approximating the structural part of ρ in (dilute) Fe containing alloys in the above alloy series as that given by $\rho(T)$ in isostructural Ni parent alloys is definitely justified. The main uncertainty in the estimation of $\rho_{mag}(T)$ then could arise from the fact that the amount of quenched disorder present in the host alloy need not be exactly the same as that in the Fe-substituted alloys, and hence making the subtraction procedure uncertain in this sense (see Sec. III).

The magnetic contribution ρ_{mag} to the resistivity in amorphous ferromagnets has been investigated theoretically by several authors.[12,13,20] Within the framework of the spin-disorder model, Richter et al.[12,13] have calculated $\rho_{mag}(T)$ for an amorphous Heisenberg ferromagnet at

both low and high temperatures, using the spin-wave (SWA) and molecular-field approximations (MFA), respectively. However, their theory treated the homogeneous case of a one-component amorphous ferromagnet, and has thus a limited applicability to the present pseudo-binary systems. Adopting a suggestion of Herzer,[31] here

we generalize the expressions for $\rho_{mag}(T)$ derived by Richter et al.[12,13] to multicomponent amorphous ferromagnets by allowing for static spin inhomogeneities. It turns out that the generalized expressions for $\rho_{mag}(T)$, i.e.,

$$\rho_{mag}^{SWA}(T)=\rho_0^c\{\langle S_i\rangle_c^2 a_3(2k_F)\left[1+\frac{\Gamma(3/2)\zeta(3/2)}{4\pi^2\langle S_i\rangle_c}\left[\frac{a^2k_BT}{D}\right]^{3/2}\right]+\frac{\pi^2}{3}\langle S_i\rangle_c\left[\frac{k_BT}{2k_F^2D}\right]^2\} \quad (\text{for } T\ll T_c) \quad (6)$$

and

$$\rho_{mag}^{MFA}(T)=\rho_0^c[\langle\langle S_i^z\rangle_T\rangle_c^2 a_3(2k_F)+\langle S_i(S_i+1)\rangle_c-\langle\langle S_i^z\rangle_T(\langle S_i^z\rangle_T+1)\rangle_c+\langle G_i^{corr}(T)\rangle_c] \quad (\text{for } T\lesssim T_c) , \quad (7)$$

where

$$\rho_0^c=\frac{3\pi}{2}\frac{m\,\Omega_c}{e^2\hbar E_F}J_{sd}^2 ,$$

$$a_n(2k_F)=(n+1)\int_0^1 d\left[\frac{q}{2k_F}\right]\left[\frac{q}{2k_F}\right]^n a_m(q) ,$$

and

$$G_i^{corr}(T)=\frac{\beta h_i\langle S_i^z\rangle_T}{\cosh(\beta h_i)-1}-\frac{2\langle S_i^z\rangle_T}{\exp(\beta h_i)-1}$$

do not differ in form from the results of Richter et al.[12,13] although some of the physical parameters take on new meanings. In these expressions S_i^z denotes the z component of a localized atomic spin $\underline{S}_i$ at position R_i, and $\langle\cdots\rangle_T$ and $\langle\cdots\rangle_c$ denote the thermal expectation value and the configurational average, respectively. Furthermore, D denotes the stiffness constant given by the magnon dispersion relation $\hbar\omega_q=Dq^2$, and Γ and ζ are the gamma- and Riemann zeta-functions, respectively. Furthermore, $\Omega_c=a^3$ is the atomic volume, k_F and E_F the Fermi wave vector and energy, J_{sd} the mean value of the sd-exchange integral, while m, e, $\hbar$, and k_B ($\beta=1/k_BT$) have their usual meanings. The spatial fluctuation of the magnetic moments is expressed in the quantity $a_3(2k_F)$, a weighted integral over the longitudinal part of the static magnetic structure factor[31]

$$a_m(q)=\frac{1}{N}\sum_{i,j}\frac{S_iS_j}{\langle S_i\rangle_c^2}\exp[-i\underline{q}(\underline{R}_i-\underline{R}_j)]-N\delta_{q,0} ,$$

which in the homogeneous case, i.e., $S_i=S_j=S$, reduces to the static geometric structure factor $a(q)$. In the expression for ρ_{mag} derived within the MFA [Eq. (7)] the effective local exchange field $H_{ex}(\underline{R}_i)$, which is related to h_i by $h_i=g\mu_BH_{ex}(\underline{R}_i)$, is left unspecified. Here, g is the Landé factor, and μ_B is the Bohr magneton.

Common to both expressions (6) and (7) is the magnetic residual resistivity

$$\rho_{mag}(0)=\rho_0^c a_3(2k_F)\langle S_i\rangle_c^2 \quad (8)$$

arising from the elastic two-center contributions, as indicated by the appearance of the averaged structure factor. In the paramagnetic region, the scattering of the conduction electrons by magnetic atoms has mainly single-site character, so that for $T\gg T_c$ the (constant) magnetic resistivity contribution

$$\rho_{mag}(T\gg T_c)=\rho_0^c\langle S_i(S_i+1)\rangle_c \quad (9)$$

contains no structural information.

Equations (6) and (7) describe the electrical resistivity in terms of magnetic quantities. Concentration dependence of the constant paramagnetic resistivity contribution [Eq. (9)] is due to that of the individual atomic spins. From the linear dependence of $\rho_{mag}(T\gg T_c)$ on x (Fig. 3) in both amorphous alloy systems one might be tempted to ascribe the paramagnetic resistivity contribution to the presence of Fe alone assuming thereby that Ni stays non-magnetic. As evidenced by recent Mössbauer and magnetization measurements[32] performed on the a-$Ni_{80-x}Fe_xB_{16}Si_4$ alloy system, this implication is definitely wrong. These investigations reveal that, while the average Fe moment (μ_{Fe}) stays essentially constant at about $1.84\mu_B$ over the composition range studied here, the average Ni moment (μ_{Ni}) rises linearly from $0.11\mu_B$ for $x=5$ to about $0.23\mu_B$ for $x=11$, and the change in the total saturation moment per $3d$ transition metal atom (μ) with alloy composition can be regarded as being entirely due to the variability of the individual Ni moments, μ_{Ni}, with respect to their environment.

No information on the individual mean magnetic moments μ_{Fe} and μ_{Ni} is presented available for the a-$Ni_{77-x}Fe_xB_{13}Si_{10}$ alloy series. However, for an estimate of these quantities one can resort to published data[26] for the Fe hyperfield (HF) and the saturation moment (μ) in these materials. μ_{Fe} then approximately follows from the phenomenological relation $HF(x)=a\mu_{Fe}(x)+b\mu(x)$, where $a\simeq12.8T/\mu_B$ and $b\simeq1.5T/\mu_B$ for the a-$Ni_{80-x}Fe_xB_{16}Si_4$ system.[32] Since the electronic structure in the two amorphous systems within the concentration range under consideration is very similar, this procedure is certainly justified. It turns out (see Table II) that also

for the a-$Ni_{77-x}Fe_xB_{13}Si_{10}$ system, the average local Fe-moment within the composition range investigated stays approximately constant at $\mu_{Fe} \simeq 1.7\mu_B$, while for $x > x_c$ Ni develops a small magnetic moment which is quite sensitive to changes in the local environment.

To investigate the theoretical linear correlation [Eq. (9)] between the paramagnetic resistivity contribution and the expectation value $\langle \underline{S}^2 \rangle$, $\rho_{mag}(T \gg T_c)$ for the investigated a-$Ni_{80-x}Fe_xB_{16}Si_4$ and a-$Ni_{77-x}Fe_xB_{13}Si_{10}$ alloys is plotted in Fig. 5 as a function of the configurationally averaged quantity $\langle S_i(S_i+1) \rangle_c$, which has been calculated using the experimentally determined average local spin quantum numbers S_i (see Table II). Figure 5 reveals that $\rho_{mag}(T \gg T_c)$ indeed exhibits a linear variation with $\langle S_1(S_1+1) \rangle_c$. This observation strongly suggests that the paramagnetic resistivity contribution $\rho_{mag}(T \gg T_c)$ is governed by the local magnetic moments and implies an almost constant strength of the sd-exchange interaction for Fe and Ni. The straight line in Fig. 5 has been obtained by Weiss and Marotta[27] for crystalline ferromagnetic $3d$ metals and alloys. From its slope $[\rho_0^c = (31.3\pm2)\mu\Omega$ cm] the parameter J_{sd} describing the strength of the sd-exchange interaction can be estimated. Assuming $E_F = (8\pm2)$ eV, $\Omega_c = (17.6\pm3)$ Å^3, and using the experimental value for ρ_0^c, one finds $|J_{sd}| = (0.75\pm0.13)$ eV, which is quite close to the commonly accepted value of about 0.5 eV (Refs. 8 and 33). In view of the approximations leading to Eq. (9), however, no serious attention should be paid to the exactness of this figure. It should also be mentioned that the strength of the sd-exchange interaction has been estimated on the basis of a free electron approximation, and should be considered as an effective strength for the combined effect of s-s and s-d scattering processes.[8] In a more rigorous derivation of the electrical resistivity of transition metals, one should evaluate the temperature-dependent transport integrals using realistic conduction-electron states.

The MFA is believed to provide a rough description
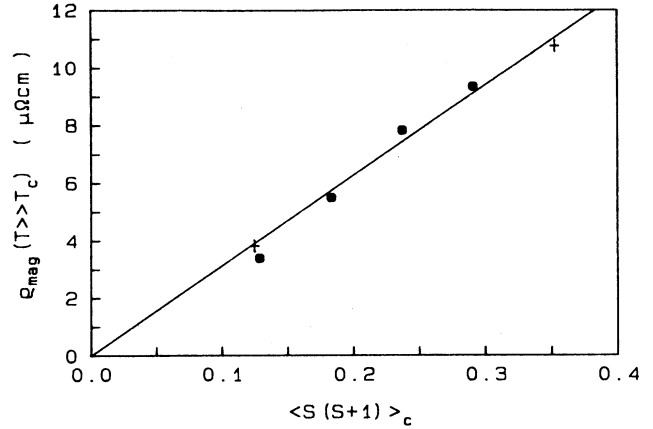
FIG. 5. Constant paramagnetic resistivity contribution $\rho_{mag}(T \gg T_c)$ of amorphous $Ni_{80-x}Fe_xB_{16}Si_4$ (closed circles) and $Ni_{77-x}Fe_xB_{13}Si_{10}$ alloys (crosses) as a function of $\langle S(S+1) \rangle_c$. The straight line through the data points has been previously determined by Weiss and Marotta (Ref. 27) for crystalline $3d$ metals and alloys.

for ρ_{mag} at intermediate temperatures, so that Eq. (7) is appropriate for explaining the experimentally observed temperature dependence and concentration dependence of ρ_{mag} for $T \lesssim T_c$. To facilitate a direct comparison with theory and between different samples the normalized resistivity ratio $\Delta r_{mag}(T) = [\rho_{mag}(T) - \rho_{mag}(0)] / [\rho_{mag}(T_c) - \rho_{mag}(0)]$ is plotted in Fig. 6 as a function of the normalized temperature T/T_c. The figure reveals that Δr_{mag} exhibits a rough linear variation with temperature for $T \lesssim T_c$, with a slope which progressively increase with decreasing Fe concentration. Expanding Δr_{mag} in powers of $(T_c - T)$ and using conventional molecular-field theory to express $\langle \langle S_i^z \rangle_T \rangle_c^2$ as a function of temperature, one obtains for $T \rightarrow T_c$

$$\Delta r_{mag}(T) \simeq 1 - \frac{10\langle S(S+1) \rangle_c}{3\langle S(S+1)(2S^2+2S+1) \rangle_c} \frac{1+\langle S(S+1) \rangle_c[\langle S^2 \rangle_c / \langle S \rangle_c^2 - a_3(2k_F)]}{\langle S(S+1) \rangle_c - a_3(2k_F)\langle S \rangle_c^2} \left[1 - \frac{T}{T_c} \right], \qquad (10)$$

which agrees with the experimentally observed linear variation of Δr_{mag} with temperature, and depends solely on the averaged magnetic structure factor $a_3(2k_F)$ and the structurally averaged magnetic quantum numbers. In order to obtain an estimate of $a_3(2k_F)$, Eq. (10) has been fitted to the $\Delta r_{mag}(T)$ data in the temperature range $0.9 \lesssim T/T_c \lesssim 1$. Values of $a_3(2k_F)$ deduced from the fitted parameters using the experimentally determined magnetic quantities S_i are listed in Table II. We note that $a_3(2k_F)$ can be quite large and decreases with increasing Fe concentration, converging to the homogeneous case $a_3(2k_F) \approx 1$. Assuming a random distribution of spins over an amorphous matrix, i.e., $a_m(q) = \langle S_i^2 \rangle_c / \langle S_i \rangle_c^2 - 1 + a(q)$, the magnitude of $a_3(2k_F)$ can

also be theoretically estimated. The calculated values for $a_3(2k_F)$ are of comparable magnitude as those determined experimentally (see Table II), and exhibit the same dependence on composition.

Let us now estimate the magnetic residual resistivity, $\rho_{mag}(0)$, which cannot be determined experimentally. According to Eq. (8), it can be calculated using the experimental values for $\rho_0^c, \langle S_i \rangle_c^2$, and the mean value for $a_3(2k_F)$. In both systems investigated, $\rho_{mag}(0)$ increases linearly with Fe content, although it contributes at most 5% to the total residual resitivity. The contribution of about 0.27 $\mu\Omega$ cm/at. Fe to the residual resistivity is considerably smaller than that to the paramagnetic resistivity contribution $\rho_{mag}(T \gg T_c)$. The MFA on the whole is
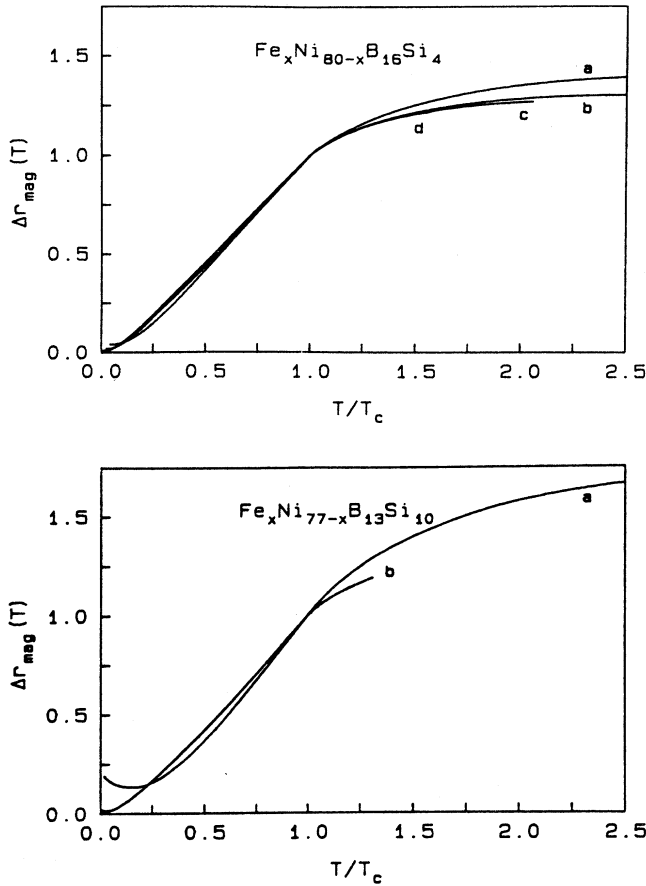
FIG. 6. Normalized incremental magnetic resistivity contribution $\Delta r_{mag}(T) = [\rho_{mag}(T) - \rho_{mag}(0)]/[\rho_{mag}(T_c) - \rho_{mag}(0)]$, of amorphous $Ni_{80-x}Fe_xB_{16}Si_4$ (above) and $Ni_{77-x}Fe_xB_{13}Si_{10}$ alloys (below) as a function of the reduced temperature T/T_c for (a) $x = 5$, (b) 7, (c) 9, (d) 11, and (a) $x = 7.7$, (b) 15.4, respectively.

found to be in fairly good agreement with the experimental results except in the paramagnetic range $(T \gtrsim T_c)$, which will be considered later.

When the temperature is lowered from T_c, the exponent of the power law gradually increases, reaching a limiting $T^{3/2}$ behavior for ρ_{mag} at low temperatures. In contrast, the theoretical low-temperature expression for ρ_{mag} [Eq. (6)] consists of two terms: one is from two competing processes, namely *incoherent* and *elastic* electron-magnon scattering, both yield a $T^{3/2}$ dependence, while the other represents the *coherent* spin-wave contribution, varying as T^2. An estimate of the relative importance of the $T^{3/2}$ and T^2 terms, assuming a $\simeq 2.6$ Å, $k_F \simeq 1.5$ Å^{-1}, and $D \simeq 50$ meV Å^2, indicates that within the temperature range investigated the $T^{3/2}$ term exceeds the T^2 term by at least 2 orders of magnitude. Thus, we have $\rho_{mag}(T) \sim T^{3/2}$ in amorphous ferromagnets for $T \ll T_c$. It remains to be seen whether the observed composition dependence of the coefficient of the $T^{3/2}$ term agrees with the theoretical expression

$$A = \rho_{mag}(0)\frac{\Gamma(3/2)\zeta(3/2)}{4\pi^2\langle S_i \rangle_c}\left[\frac{a^2 k_B}{D}\right]^{3/2},$$

and whether the magnitude of A is also reasonable. Values for A calculated from this relation, using $a \simeq 2.6$ Å and the experimental data for $\rho_{mag}(0)$, $\langle S_i \rangle_c$ and D, are given in Table II along with the corresponding experimental data. From these values, it is evident that the theoretical values for A are within a factor of 2–4 of those of the experiment, and exhibit the same dependence on the composition. The fact that the difference between the theory and the experiment for both systems investigated are of the same order can be taken to be an additional justification for the averaging during the estimation of $a_3(2k_F)$. At low Fe concentrations it is just the magnitude of $a_3(2k_F)$ that pushes the theoretical values for A close to the experimental ones. However, the remaining discrepancy between the calculated and experimental values for A can be traced to the breakdown of the MFA in the critical region, where the $\Delta r_{mag}(T)$ data have been fitted to Eq. (10) in order to arrive at a numerical estimate for $a_3(2k_F)$. Consequently, the spin-disorder model appears to be remarkably successful in accounting *quantitatively* for the $\rho_{mag}(T)$ behavior in the diluted amorphous ferromagnetic alloys investigated here if allowance is made for static spin inhomogeneities in the theoretical electronic transition rates. In this sense, the present results unambiguously justify the decomposition of the resistivity according to Matthiessen's rule, as well as the assumption of dominant s-band contributions to the conductivity within the range of purity studied here.

The low-temperature $T^{3/2}$ dependence for ρ_{mag} obtained here for *diluted* glassy ferromagnetic alloys differs considerably from our earlier data[9] for *concentrated* Fe-rich amorphous ferromagnets, which exhibit a T^2 low-temperature behavior for ρ_{mag}. The reason for the difference is that in the former case, due to the small number of moment-bearing (Fe) atoms, the *inelastic, incoherent* scattering of electrons from long-wavelength spin waves dominates over the *inelastic, coherent* spin-wave scattering as well as the *elastic* scattering from the randomly distributed temperature-dependent local spin inhomogeneities. With increasing Fe concentration, the *elastic* spin-disorder scattering contribution starts to become comparable to that from the *inelastic, incoherent* spin-wave scattering, so that for concentrated (Fe-rich) amorphous alloys these contributions (both varying as $T^{3/2}$, but having different signs) are roughly of the same magnitude and almost cancel each other, leaving the *inelastic, coherent* spin-wave contribution, which varies as T^2.

However, deeper physical understanding of these interrelations requires certain refinements of the transport model used so far that, e.g., completely disregards the spin splitting of the conduction band giving rise to marked deviations from Matthiessen's rule in crystalline ferromagnetic alloys.[14,15] Due to exchange splitting of these sub-bands, the properties of electrons near the Fermi level depend on their spin direction, and in particular spin-flip scattering (such as electron-magnon scattering) can contribute to the total resistivity by transferring electrons between sub-bands. On the basis of a combined spin and potential scattering, Herzer[31] has recently generalized this TCC model to amorphous ferromagnets.

The expression derived for the total resistivity can be written as follows:

$$\rho(T) \simeq \rho_0 + 2 \frac{(1+\alpha^2)}{(1+\alpha)^2} \rho_{\text{mag}}(T) + \left[\frac{1-\alpha}{1+\alpha} \right]^2 \rho_{\text{mag}}^{\uparrow\downarrow}(T) , \quad (11)$$

where, apart from a small temperature-dependent contribution, ρ_0 represents the (structural) residual resistivity, $\rho_{\text{mag}}(T)$ according to the temperature range is identical to Eq. (6) or (7), and $\rho_{\text{mag}}^{\uparrow\downarrow}(T)$ is a mixing term that can be neglected within the MFA. In the spin-wave region $\rho_{\text{mag}}^{\uparrow\downarrow}(T)$ is given by

$$\rho_{\text{mag}}^{\uparrow\downarrow}(T) = \rho_0^c \langle S_i \rangle_c \left[\frac{3\Gamma(3/2)\zeta(3/2)}{2\pi^2} [a_1(2k_F) - a_3(2k_F)] \left[\frac{a^2 k_B T}{D} \right]^{3/2} + \frac{k_B T}{k_F^2 D} \left[I_1(y_{\text{min}}) - \frac{k_B T}{2k_F^2 D} I_{3/2}(y_{\text{min}}) \right] \right] , \quad (12)$$

where

$$I_n(y) = \int_{y_{\text{min}}}^{\infty} dx \frac{(x-y)^{n-1} e^x}{(e^x - 1)^2}$$

and $y_{\text{min}} = \beta(\Delta/E_F)^2 D k_F^2$ ($\Delta = J_{sd} \langle \langle S_i^z \rangle_T \rangle_c$), which takes into account that for the coherent scattering of the conduction electrons from the $s\uparrow$ to the $s\downarrow$ sub-band (and for the reverse process) a minimum momentum $q_{\text{min}} = |k_F^{\uparrow} - k_F^{\downarrow}|$ is required.

According to Eq. (11) the temperature dependence of ρ is critically dependent on the residual resistivity ratio $\alpha = \rho_0^{\downarrow}/\rho_0^{\uparrow}$. In view of the low magnetic moment[26,32] and high density of states at the Fermi level[23,24] the present glassy alloys can be considered to be weak itinerant ferromagnets with $\alpha \approx 1$, so that the contribution of the mixing term to ρ in Eq. (11) should be negligibly small. Equation (11) then reduces to the one-current conduction model [Eq. (6)] used in our analysis, thus leaving all conclusions unchanged. With increasing Fe concentration, however, amorphous $3d$ transition metal-metalloid alloys tend to become strong ferromagnets[34] (i.e., α starts increasing from 1), and hence the mixing term in Eq. (11) comes into play. Since the factor $[a_1(2k_F) - a_3(2k_F)]$ of the $T^{3/2}$ term in Eq. (12), which strongly depends on the magnetic short-range order and for a dense random packing of magnetic atoms is negative as well as near unity, in concentrated amorphous (nearly strong or strong itinerant) ferromagnets it almost compensates the corresponding $T^{3/2}$ contribution of the second term in Eq. (11). Consequently, in agreement with our previous interpretation of the experimental results, the TCC model predicts that in Fe-rich amorphous alloys the inelastic, coherent T^2 spin-wave scattering contribution should become increasingly important at the expense of the inelastic, incoherent, and elastic scattering contributions as α increases.

We now return to the behavior of ρ_{mag} in the critical and paramagnetic regions. While the conventional MFA [Eq. (7)] correctly predicts the variation of ρ_{mag} with temperature for $T \lesssim T_c$, it fails to account for the marked temperature dependence of ρ_{mag} for $T \geq T_c$ (Fig. 6). Because of the single-site character of the MFA in the paramagnetic range, this failure is not unexpected. In the vicinity of the ordering temperature, critical scattering of the conduction electrons on the fluctuations of the spin-

system is the dominant mechanism and governs the transport processes.[35]

In the diagram for $\Delta r_{\text{mag}} = f(T/T_c)$ (Fig. 6), the slope of Δr_{mag} for $T \lesssim T_c$ varies only slightly with alloy composition, whereas above T_c the curves fan out strongly. This effect is very pronounced for the $B_{13}Si_{10}$ alloy series. The considerable variation of ρ_{mag} in the paramagnetic range clearly demonstrates the persistence of short-range magnetic ordering in these materials over a wide range of temperatures above T_c, a fact which is also corroborated by recent Mössbauer measurements[36] on similar metallic glasses, and is basically responsible for the nonmonotonous variation of the critical exponent γ of magnetic initial susceptibility.[37] Keeping in mind that the slope of ρ_{mag} in the spin-wave region is considerably enhanced through the appearance of the weighted integral over the static magnetic structure factor in the theoretical $\rho_{\text{mag}}(T)$ expression, in the paramagnetic region the magnitude of $d\rho_{\text{mag}}/dT$ should likewise be dictated by the present short-range magnetic order. Thus, in excellent agreement with the experimental results, $d\rho_{\text{mag}}/dT$ should assume the largest values for those compositions exhibiting lowest ordering temperatures. Moreover, in both amorphous alloy systems investigated the ratio $\Delta r_{\text{mag}}(T \gg T_c)/\Delta r_{\text{mag}}(T_c)$ progressively decreases with increasing Curie temperature, and concurrently the reduced temperature range $\epsilon = |T - T_c|/T_c$, in which short-range correlations of the spin system persist, becomes narrower approaching the width expected for homogeneous crystalline ferromagnets. Whereas in pure crystalline ferromagnets short-range spin correlations die out rapidly within $\epsilon < 0.1$ (Ref. 35), in the present amorphous alloys it may extend up to $\epsilon = 3$. In this sense, diluted magnetic glasses exhibit a unique $\rho_{\text{mag}}(T)$ behavior in the paramagnetic range.

Besides the peculiarities of magnetic resistivity contribution ρ_{mag} in diluted amorphous ferromagnets above the transition temperature, in these materials there are also striking deviations from the $\rho_{\text{mag}}(T)$ behavior normally observed in homogeneous crystalline ferromagnets in the asymptotic critical region. While in crystalline systems,[35] in the immediate vicinity of Curie point, $d\rho_{\text{mag}}/dT$ exhibits the typical λ-shaped pattern, which is characteristic also for the magnetic specific heat capacity C_{mag}, in the diluted amorphous ferromagnets investigated $d\rho/dT$

shows only a very weak singularity at T_c (see Figs. 1 and 2). Assuming that the real critical region in the amorphous systems is of comparable size as that of the crystalline ferromagnets, i.e., $\epsilon = |T - T_c|/T_c \lesssim 0.03$ (Ref. 34), we should be able to detect an increase of $d\rho_{mag}/dT$ in the ferromagnetic range as $T \to T_c$, at least for those compositions with the highest ordering temperatures. Thus, if such an increasing of $d\rho_{mag}/dT$ is present at all, it must be confined to an interval of at least $(T_c - T) < 1$ K. Finally, we mention that attempts to take advantage of the proportionality between the magnetic contribution to specific heat, C_{mag}, and $d\rho_{mag}/dT$ in the critical region[36] to obtain the asymptotic critical exponent α and the ratio of critical amplitudes from the $d\rho/dT$ data have turned out to be unsuccessful, because of insufficient knowledge of the resistivity behavior within the critical region.

V. CONCLUSIONS

The resistivity characteristics of amorphous ferromagnets is due to a complicated interplay of various scattering mechanisms. It was shown that for the diluted amorphous ferromagnets investigated the contribution ρ_{mag} produced by spin scattering can be separated in the whole temperature range only assuming the validity of Matthiessen's rule. The magnetic contribution, ρ_{mag}, to the resistivity is small compared to the structural one, but it essentially determines the temperature dependence of the total resistivity in the ferromagnetic range. Analysis of ρ_{mag} within the spin-disorder model allows the following conclusions to be made: (i) the constant paramagnetic resistivity contribution $\rho_{mag}(T \gg T_c)$ is governed by the individual average local magnetic moments, (ii) the quenched disorder does not exert any noticeable influence on the resistivity quantity ρ_0^c characteristic for $3d$ metals and alloys, (iii) at $T \leq T_c$, both magnitude as well as concentration and temperature dependence of ρ_{mag} are in satisfactory agreement with the theoretical predictions if the amorphous structure is taken into account by allowing for static spin inhomogeneities in calculating the electronic transition rates for spin scattering, (iv) the difference of ρ_{mag} in the paramagnetic range compared to that at T_c, which cannot be explained within the simple MFA, is associated with the spin inhomogeneities, which also govern the magnitude of ρ_{mag} in the ferromagnetic range, and (v) $d\rho/dT$ exhibits only a very weak singularity at T_c, which does not allow the extraction of the asymptotic value of the critical exponent α of the specific heat.

[1]K. V. Rao, in *Amorphous Metallic Alloys*, edited by F. E. Luborsky (Butterworths Monographs in Materials, 1983), p. 401.

[2]Z. Marohnic, K. Saub, E. Babic, and J. Ivkov, Solid State Commun. **30**, 651 (1979).

[3]G. Böhnke and M. Rosenberg, J. Phys. (Paris) Colloq. **41**, C8-481 (1980).

[4]G. Thummes, R. Ranganathan, and J. Kötzler, Z. Phys. **157**, 699 (1988); G. Thummes, J. Kötzler, R. Ranganathan, and R. Krishnan, Z. Phys. B **69**, 489 (1988).

[5]W. H. Kettler and M. Rosenberg, J. Phys. F **17**, L209 (1987).

[6]T. Kasuya, Prog. Theor. Phys. (Kyoto) **22**, 227 (1959).

[7]I. Mannari, Prog. Theor. Phys. (Kyoto) **22**, 335 (1959).

[8]D. A. Goodings, Phys. Rev. **132**, 542 (1963).

[9]S. N. Kaul, W. H. Kettler, and M. Rosenberg, Phys. Rev. B **33**, 4987 (1986).

[10]P. J. Cote and L. V. Meisel, in *Glassy Metals I: Ionic Structure, Electronic Transport and Crystallization*, edited by H.-J. Güntherodt and H. Beck (Springer-Verlag, Berlin, 1981), p. 141.

[11]E. Babic, Z. Marohnic, M. Ocko, A. Hamzic, K. Saub, and B. Pivac, J. Magn. Magn. Mater. **15**, 934 (1980).

[12]R. Richter, M. Wolf, and F. Goedsche, Phys. Stat. Sol. B **95**, 473 (1979).

[13]R. Richter and F. Goedsche, Phys. Stat. Sol. B **123**, 143 (1984).

[14]I. A. Campbell and A. Fert, in *Ferromagnetic Materials*, edited by E. P. Wohlfarth (North-Holland, Amsterdam, 1982), Vol. 3, p. 747.

[15]F. Goedsche, A. Möbius, and A. Richter, Phys. Stat. Sol. B **96**, 279 (1979).

[16]N. F. Mott, Adv. Phys. **13**, 325 (1964).

[17]L. E. Ballentine, in *Rapidly Quenched Metals V*, edited by S. Steeb and H. Warlimont (North-Holland, Amsterdam, 1985), p. 981.

[18]H. Ostermeier, W. Fembacher, and U. Krey, Z. Phys. **157**, 489 (1988).

[19]K. Aso, M. Hayakawa, K. Hotai, S. Uedaira, Y. Ochiai, Y. Makino, *Proceedings of the 4th International Conference on Rapidly Quenched Metals*, Sendai, 1981, edited by T. Masumoto and K. Suzuki (Japan Institute of Metals, Sendai, 1982).

[20]S. Skalski, M. P. Kawatra, J. A. Mydosh, and J. I. Budnick, Phys. Rev. B **9**, 3613 (1970).

[21]G. Williams, J. Phys. Chem. Solids **31**, 529 (1970).

[22]G. Williams, and J. W. Loram, J. Phys. Chem. Solids **30**, 1827 (1969).

[23]M. Regelsberger, M. Rosenberg, and R. Wernhardt, J. Appl. Phys. **57**, 3551 (1985).

[24]U. Mizutani and M. Takeuchi, J. Phys. F **16**, 79 (1986).

[25]B. Borgmeier, Diplom thesis, Ruhr-Universität Bochum, 1987.

[26]G. Hilscher, R. Haferl, H. Kirchmayr, M. Müller, H.-J. Güntherodt, J. Phys. F **11**, 2429 (1981).

[27]R. J. Weiss and A. S. Marotta, J. Phys. Chem. Solids **9**, 302 (1959).

[28]W. Kierspe, R. Kohlhaas, and H. Gonska, Z. Angew, Phys. **24**, 28 (1967).

[29]E. Esposito, H. Ehrenreich, and C. D. Gelatt, Jr., Phys. Rev. B **18**, 3913 (1978).

[30]G. Bergmann and P. Marquardt, Phys. Rev. B **17**, 1355 (1978).

[31]G. Herzer, Ph.D. thesis, University of Stuttgart, 1983; J. Magn. Magn. Mater. **45**, 345 (1984).

[32]P. Deppe, T. S. Park, L. Ressler, M. Rosenberg, and M. Sos-tarich, in *Rapidly Quenched Metals V*, edited by S. Steeb and H. Warlimont (North-Holland, Amsterdam, 1985), Vol. II, p. 1227.

[33]R. Hasegawa and C. C. Tsuei, Phys. Rev. B **2**, 1631 (1970); A. K. Nigam and A. K. Majumdar, Phys. Rev. B **27**, 495 (1983).

[34]S. N. Kaul and M. Rosenberg, Phys. Rev. B **27**, 5698 (1983).

[35]M. Ausloos, in *Magnetic Phase Transitions*, edited by M. Ausloos and R. J. Elliot (Springer-Verlag, Berlin, 1983), p. 99.

[36]H. J. Eickelmann, M. M. Abd-Elmeguid, H. Micklitz, and R. A. Brand, Phys. Rev. B **29**, 2443 (1984).

[37]S. N. Kaul, J. Magn. Magn. Mater. **53**, 5 (1985).